Inorganic Chemistry

Article

pubs.acs.org/IC

Understanding Lanthanoid(III) Hydration Structure and Kinetics by Insights from Energies and Wave functions

Jun Zhang,* Norah Heinz, and Michael Dolg*

Institute for Theoretical Chemistry, University of Cologne, Greinstr. 4, D-50939 Cologne, Germany

Supporting Information

ABSTRACT: The hydration of all trivalent lanthanoid (Ln) ions is studied theoretically from two aspects: energy and wave function. With the help of the incremental scheme, for the first time the lanthanoid(III) aqua complexes are computed at the CCSD(T) level using large basis sets. These computations prove that SCS-MP2 is nearly as accurate as CCSD, thus enabling us to give the most accurate first principle hydration Gibbs free energies and reliable preferred coordination numbers (CNs) of lanthanoid(III) aqua complexes: 9, 8, and both, for light, heavy, and intermediate lanthanoids, respectively. Then a series of wave function analyses were performed to explore the deeper reasons for the preference of specific CNs. An unexpected observation is that as Ln goes from samarium to lutetium, the capping Ln−O bonds in nona-aqua lanthanoid complexes become weaker while they get shorter. Therefore, as the capping Ln−O bonds are getting easier to disrupt, heavier lanthanoids will prefer a low CN, i.e., 8. On the basis of this and previous work of other groups, a model for the water exchange kinetics of lanthanoid(III) ions is proposed. This model suggests that the capping Ln−O bonds of moderate strength, which occur for intermediate lanthanoids, are advantageous for the formation of a bicapped trigonal prism intermediate during water exchange. This explains some NMR experiments and, more importantly, an observation which puzzled investigators for a long time, i.e., that the exchange rate reaches a maximum for the middle region but is low at the beginning and end of the lanthanoid series. This nontrivial behavior of capping Ln−O bonds is interpreted and is believed to determine the hydration behavior of lanthanoid(III) ions.

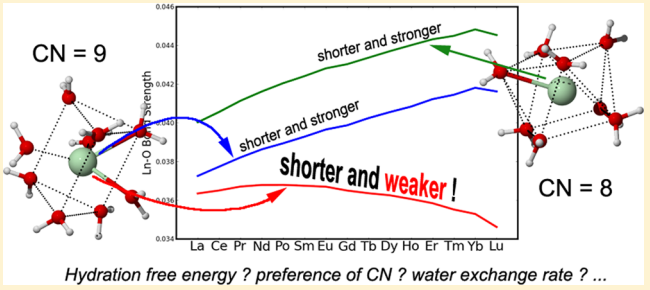

INTRODUCTION

Ionic hydration is a fundamental phenomenon in nature, determining the solvation dynamics, chemical reactivity, and several biological as well as industrial processes. Of the numerous possible atomic cations and anions, the hydration of trivalent lanthanoid ions (Ln^{3+}) has been an active subject of research for a long time since it is involved in many practical applications. For the extraction and separation of lanthanoids, hydration energies and kinetics are necessary quantities to calculate the relative selectivities and binding rates in the development of effective extracting ligands or solvents.[1,2] In magnetic resonance imaging gadolinium(III) complexes are often used as contrast agents[3,4] and the hydration of gadolinium(III) directly determines the relaxation enhancement imaging mechanism.[5]

The lanthanoid(III) hydration is also of academical interest because the very subtle changes in electronic structures from La^{3+} to Lu^{3+} nevertheless induce quite complex hydration behaviors.[6] It is accepted that the number of water molecules in the first hydration shell, i.e., the coordination number (CN), is 9 and 8 for light (e.g., La^{3+}, Ce^{3+}) and heavy (e.g., Yb^{3+}, Lu^{3+}) lanthanoids, respectively.[6] From Figure 1 we see that the octa- and nona-lanthanoid(III) aqua complexes possess a square antiprism (SAP) and tricapped trigonal prism (TTP) structure.[6] The latter contains two kinds of Ln−O bonds: six prism (oxygen atoms on the vertices of the trigonal prism, called "Ln−O(9P)" hereafter) and three capping ones ("Ln−O(9C)"). In analogy the Ln−O bonds in octa-aqua lanthanoid(III) complexes are called "Ln−O(8)" for convenience. The preferred CNs of intermediate lanthanoids are more difficult to determine, and early studies often produced conflicting results. For instance, investigators used to believe the existence of a "gadolinium break", i.e., a sudden change of the preferred CN at Gd^{3+}.[7,8] However, recent experiments found no such discontinuous change in CNs, and the relative stabilities between nona- and octa-aqua lanthanoid(III) complexes show a progressive change in aqueous solution.[9,10] Thus, for these intermediate lanthanoids their CNs should be averaged according to the ratio of nona- and octa-aqua forms, being a noninteger. Moreover, lanthanoids(III) exhibit very strange hydration kinetics: the exchange rate of the water molecules between the first hydration sphere and the bulk solvent increases from La^{3+} to Gd^{3+} and decreases thereafter to Lu^{3+}; i.e., it reaches maximum in the middle region of the lanthanoid series.[11,12] The physical reasons for these phenomena are not well understood. For more details of the fascinating lanthanoid-

Received: April 29, 2014
Published: June 24, 2014

   dx.doi.org/10.1021/ic500991x | Inorg. Chem. 2014, 53, 7700−7708

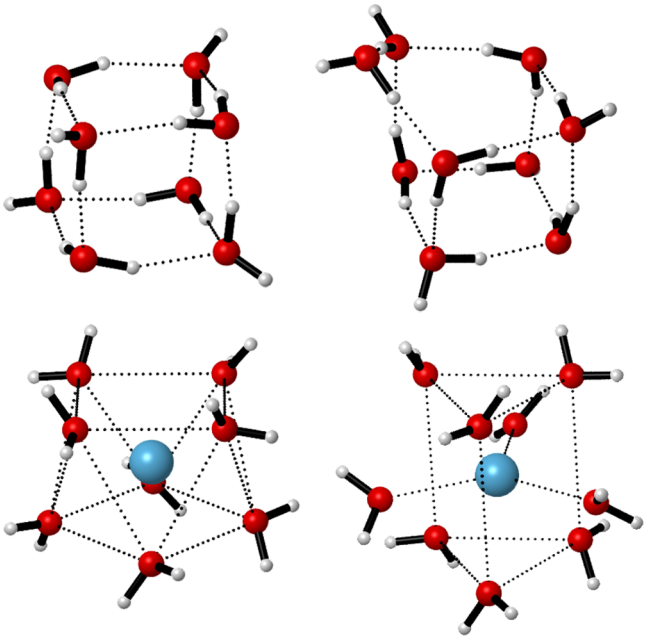

Figure 1. Geometries of water clusters $(H_2O)_n$ and lanthanoid(III) aqua complexes $Ln(H_2O)_n^{3+}$ (n = 8, 9).

(III) hydration behavior, the reader is referred to several reviews.[6,9,11]

Modern experimental studies of lanthanoid(III) hydration are nearly always coupled with theoretical methods. The X-ray absorption spectroscopy (XAS) method is the most important one in unraveling lanthanoid(III) hydration, and the interpretation of its results must rely on some models and simulations.[10,13,14] From a pure theoretical point of view, molecular dynamics (MD) and quantum chemistry (QC) have both been applied to this field. The advent of polarizable force fields for lanthanoids(III)[15,16] has enabled classical MD studies to be highly accurate, from which dynamical information can be extracted. For QC one should realize that the large number of electrons, strong relativistic effects, and incomplete 4f shell occupation in lanthanoids make their study quite difficult. Nevertheless, the development of effective core potentials (ECP)[17] which implicitly takes those aspects into account significantly improves the computational ability for lanthanoids. The large- and small-core energy-consistent pseudopotentials (PPs) developed in our group for lanthanoids[18−20] have proven to be both accurate and efficient. Both sets of PPs were applied in studies of lanthanoid(III) hydration.[21−24] The most accurate QC study so far was performed by Ciupka et al.[24] In that work all $Ln(H_2O)_n^{3+}$ complexes with n = 7, 8, 9 were optimized with large basis sets at the correlated MP2 level in the gas phase. The experimental Ln−O bond lengths are quite well reproduced. With thermodynamical and solvent effects taken into account, the hydration Gibbs free energies were calculated to be about 50 kJ/mol within the experimental ones.[25] Moreover, the preferred CN for each Ln^{3+} was determined and compared with the experimental results.

While density functional theory (DFT) and (SCS-)MP2[26] have been applied to the lanthanoid(III) aqua complexes,[21−24] the intrinsic accuracy of these methods remains unknown, because a benchmark with a highly accurate ab initio method such as CCSD(T) used to be impossible due to the large computational effort. Fortunately, in the last several years our group's work based on the incremental scheme[27−29] made the CCSD(T) computation of systems of such size feasible, while keeping a sufficiently high accuracy. Therefore, we decided to perform CCSD(T) calculations on $Ln(H_2O)_n^{3+}$ (n = 8, 9) in the gas phase to produce very accurate results as well to as examine the reliability of the previous studies. Meanwhile, up to now most QC studies have focused only on the geometries and energies. In order to get deeper insight into the electronic structures of these lanthanoid(III) aqua complexes, we performed a variety of wave function analyses, such as atom-in-molecule (AIM) theory.[30] We will see that these properties other than the energy reveal valuable and unexpected information for these aqua complexes, enabling us to explain the preference of CNs and the strange trend of the water exchange rates.

METHODS

In this work we studied the octa- and nona-aqua lanthanoid(III) complexes, i.e., $Ln(H_2O)_8^{3+}$ and $Ln(H_2O)_9^{3+}$, with Ln = La to Lu. The free Ln^{3+} ions as well as the water clusters $(H_2O)_8$ and $(H_2O)_9$ were also considered. For hydrogen and oxygen aug-cc-pVTZ basis sets were used.[31] For the lanthanoids, the core−shell electrons were substituted by scalar-relativistic 4f-in-core PPs.[18] The valence electrons were represented by (8s7p6d3f2g)/[6s5p5d3f2g] GTO basis sets, which contain a set of (2s1p1d) diffuse and (3f2g) polarization functions.[32] The geometries optimized at the MP2 level were obtained from ref 24 and are shown in Figure 1.

CCSD(T) energy calculations were performed for all species mentioned above at the MP2 optimized geometries. Despite the usage of PPs the number of correlated electrons and orbitals is up to 80 and 900, respectively, which is beyond our computational ability for standard CCSD(T) calculations in C_1 symmetry. Therefore, we performed CCSD(T) through our recently developed third-order incremental dual basis-set zero-buffer approach[29,33] (inc3-db-B0). In brief, this method decomposed the octa- and nona-aqua lanthanoid-(III) complexes into 9 and 10 "domains", respectively, each domain being a water molecule or lanthanoid ion. Then we performed CCSD(T) calculations for each domain as well as unions of up to three domains and combined the results by the incremental scheme (inc3) to obtain the total energies. The dual basis-set zero-buffer (db-B0) strategy can reduce the computational cost considerably without significant loss of accuracy. Although calculations with the incremental scheme are more costly than the application of other local correlation

Table 1. Binding Energies (Unit: kJ/mol) Computed by inc3-db-B0-, OSV-, and DLPNO-CCSD(T)[a] for Small Water Clusters[b]

method	standard	inc3-db-B0	inc2-db-B0	OSV	DLPNO
$(H_2O)_6$(cage)	−272.29	−272.18	−271.62	−254.60	−266.54
$(H_2O)_6$(prism)	−280.26	−280.11	−279.53	−262.27	−273.34
$(H_2O)_8(D_{2d})$	−426.40	−426.23	−424.89	−397.89	−417.35
$(H_2O)_8(S_4)$	−426.72	−426.56	−425.28	−398.15	−419.11
$(H_2O)_9$	−446.89	−446.49	−444.53	−413.02	−436.81

[a]All calculations are performed with cc-pVDZ basis set. OSV- and DLPNO-CCSD(T) calculations were performed by Molpro 2012.1[39] and ORCA 3.0.1,[40] respectively. [b]Geometries are obtained from literature. Hexamers: ref 36; octamers: ref 37; nonamer: ref 38.

dx.doi.org/10.1021/ic500991x | Inorg. Chem. 2014, 53, 7700−7708

Table 2. Hydration Gibbs Free Energies (Unit: kJ/mol) of Lanthanoid(III) Aqua Complexes

	$Ln(H_2O)_8^{3+}$			$Ln(H_2O)_9^{3+}$			hydration free energy	
Ln	D_e[a]	ΔE_c[b]	ΔG_H[c]	D_e[a]	ΔE_c[b]	ΔG_H[c]	computed[d]	expt[e]
La	1623.22	−1497.77	−3171.63	1700.46	−1431.69	−3187.01	3187	3145
Ce	1655.45	−1495.07	−3201.16	1732.30	−1429.54	−3216.71	3217	3200
Pr	1686.20	−1496.67	−3233.51	1761.90	−1431.47	−3248.23	3248	3245
Nd	1715.07	−1499.12	−3264.83	1789.50	−1433.43	−3277.78	3278	3280
Pm	1742.35	−1501.76	−3294.75	1815.36	−1436.88	−3307.10	3307	3250
Sm	1768.67	−1504.98	−3324.28	1840.28	−1440.67	−3335.82	3336	3325
Eu	1794.97	−1508.49	−3354.10	1865.43	−1444.26	−3364.55	3364	3360
Gd	1819.60	−1508.58	−3378.82	1888.01	−1445.08	−3387.95	3388	3375
Tb	1845.37	−1509.56	−3405.57	1911.99	−1446.24	−3413.09	3413	3400
Dy	1869.86	−1511.79	−3432.29	1934.58	−1448.40	−3437.84	3437	3425
Ho	1893.78	−1513.92	−3458.33	1956.50	−1451.55	−3462.90	3462	3470
Er	1917.43	−1516.04	−3484.11	1978.26	−1453.05	−3486.18	3486	3495
Tm	1939.10	−1519.74	−3509.48	1998.08	−1455.49	−3508.43	3509	3515
Yb	1961.28	−1522.24	−3534.16	2018.82	−1459.37	−3533.05	3534	3570
Lu	1975.43	−1530.19	−3556.26	2031.15	−1467.09	−3553.09	3556	3515

[a] D_e: The gas phase binding energy computed at CCSD(T) level in this work. [b] ΔE_c: The sum of zero point energy changes, solvent effect, entropy contribution, and standard state correction at (SCS-)MP2 level in ref 24. See the Supporting Information for details. [c] ΔG_H: The hydration free energy, computed as $\Delta G_H = -D_e + \Delta E_c + EHBC$, where $EHBC = -4.22k$. For $n = 8$ and 9, $k = 12$ and 13, respectively. [d] Obtained by averaging ΔG_H of octa- and nona-aqua lanthanoids in Table 2 with a Boltzmann factor $\exp(-\Delta G_H/RT)$, where $T = 298.15$ K. [e] The experimental results are taken from ref 25.

methods, they have the virtue of being also more accurate and can easily be parallelized. In fact we proved that for relative energies of various classes of chemical systems the difference between inc3-db-B0-CCSD(T) and standard CCSD(T) is less than 1.94 kJ/mol.[29] To confirm this in the case of the hydration problem, we compared the accuracy of inc3-db-B0-CCSD(T) with that of two other state-of-the-art local correlation methods, i.e., orbital-specific-virtual (OSV)[34] and domain based local pair-natural orbital (DLPNO) CCSD(T),[35] on water clusters $(H_2O)_n$ (n = 6, 8, and 9).[36−38] We computed the binding energies according to the reaction $nH_2O \rightarrow (H_2O)_n$ and compared the results to those from standard CCSD(T) reference calculations. The results are listed in Table 1.

The inc3-db-B0 approach is found to be the most accurate one with an error of less than 1.0 kJ/mol for all cases. Even the inc2-db-B0 is much better than the OSV and DLPNO approaches. Because we are aiming at the highest possible accuracy, the inc3-db-B0 approach will be used. Further details of this approach are summarized in our recent works.[29,33] All calculations were performed with the in-house C++ incremental code and Molpro 2012.1.[39]

For the wave function analysis, self-consistent field (SCF) wave functions computed by hybrid B3LYP functional[41] obtained with Gaussian03[42] were used. The evaluation of the electron localization function (ELF),[43] bond order analysis, and AIM properties[30] was then carried out by Multiwfn 3.2.[44]

■ ENERGY COMPUTATIONS

Gas Phase Binding Energies. We computed the binding energies according to the following reaction in the gas phase:

$$Ln^{3+}(g) + (H_2O)_n(g) \rightarrow Ln(H_2O)_n^{3+}(g) \quad (n = 8, 9) \tag{1}$$

A comprehensive collection of the computed HF, B3LYP, CCSD, and CCSD(T) energies in this work and the MP2 and SCS-MP2 energies obtained from ref 24 are listed in Tables S1 and S2 of the Supporting Information. In Table 2 we only list CCSD(T) energies, and in Table 3 and Figure 2 we show the errors of the other methods with respect to the CCSD(T) reference. We observe that MP2 and CCSD overestimate the binding energies by about 35 and 5 kJ/mol, respectively, and the errors for octa- and nona-aqua ions are almost identical. In

Table 3. Binding Energy Root-Mean-Square-Deviations (RMSDs) (Unit: kJ/mol) with Respect to CCSD(T) for All Considered Methods

method	$Ln(H_2O)_8^{3+}$	$Ln(H_2O)_9^{3+}$
HF	3.05	12.71
MP2[a]	35.09	32.06
CCSD	5.72	5.19
B3LYP	15.64	37.62
SCS-MP2[a]	5.13	5.11

[a] The binding energies are taken from ref 24.

contrast B3LYP underestimates the binding energies and exhibits size-dependent errors. For octa-aqua ions its error (15.64 kJ/mol) is much smaller than for MP2, and for nona-aqua ions (37.62 kJ/mol) slightly larger. A similar trend is observed in the case of $SO_4^{2-}(H_2O)_n$ clusters:[45] as n increases from 3 to 6, the binding energy error of MP2 changes from 1.33 to 4.64 kJ/mol, whereas that of B3LYP increases drastically from 1.17 to 26.48 kJ/mol. These observations suggest that, for these aqua complexes, the error of traditional DFT, at least for B3LYP, increases with the system size, whereas MP2 is more robust.

Astonishingly, the accuracy of HF is better than the one of MP2 and B3LYP. However, the unsystematic behavior of errors reflects that this is an example of "right answer for wrong reason", i.e., a lucky error cancellation. SCS-MP2 shows an excellent performance, comparable with the one of CCSD, however the error changes from an overestimation at La gradually to an underestimation at Lu. Splitting the MP2 correlation energy contribution to the energy change of reaction 1 into triplet and singlet components suggests that the triplet component always favors reaction 1, whereas the singlet component always disfavors it (see Table S3 of the Supporting Information), implying the former being overestimated or/and the latter underestimated. This is exactly what the spin-component-scaling (SCS) approach tries to correct

dx.doi.org/10.1021/ic500991x | Inorg. Chem. 2014, 53, 7700−7708

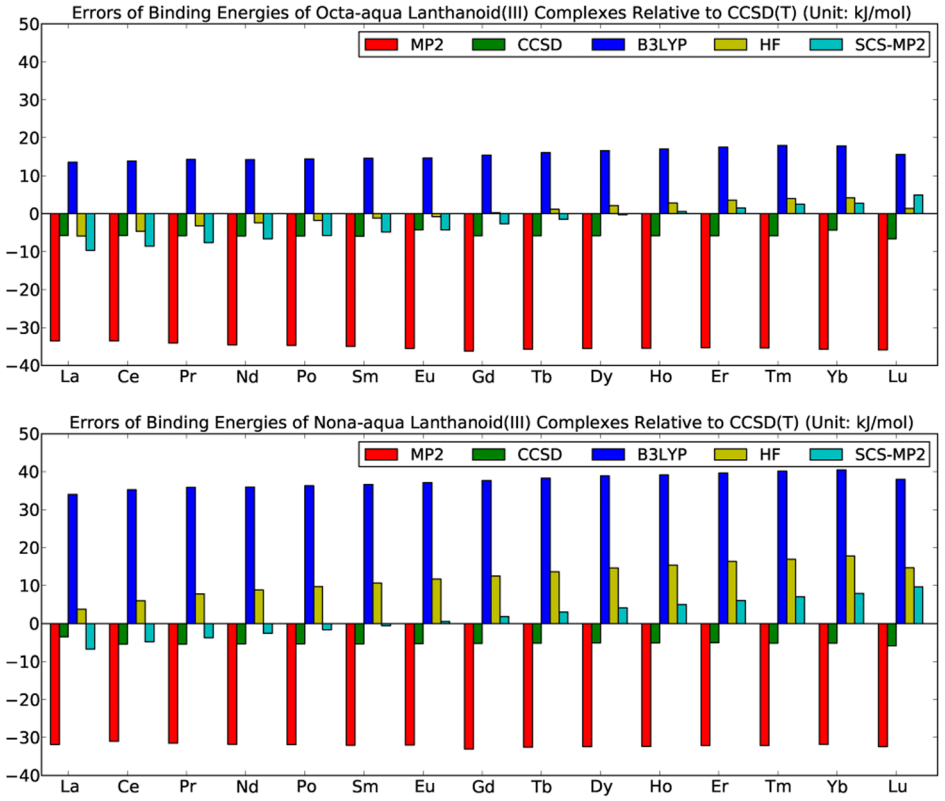

Figure 2. Binding energy errors (unit: kJ/mol) with respect to CCSD(T) for all considered methods. The errors of method X here are defined as $D_{CCSD(T)}-D_X$, where D_X is the binding energy computed by method X.

and the physical reason why SCS-MP2 improves MP2 here significantly.

We also examined the magnitude of the basis set superposition error (BSSE) at the CCSD(T) level by using the counterpoise (CP) correction[46] for Gd^{3+} aqua complexes. The results turn out to be 5.27 and 5.07 kJ/mol for $Gd(H_2O)_8^{3+}$ and $Gd(H_2O)_9^{3+}$, respectively, being less than 0.3% of the binding energy. Thus, the accuracy of the basis sets used in this study is sufficiently high to avoid a large BSSE at the correlated level. Since the magnitudes of BSSEs for all the lanthanoid(III) aqua complexes should be similar, we do not think that it is necessary to compute CP corrections for all the complexes.

Hydration Gibbs Free Energies. In order to get the hydration Gibbs free energy of lanthanoids(III) for the reaction

$$Ln^{3+}(g) + (H_2O)_n(aq) \rightarrow Ln(H_2O)_n^{3+}(aq) \quad (n = 8, 9) \tag{2}$$

thermodynamical and solvent effects must be taken into account. These quantities have already been calculated in ref 24 at the (SCS-)MP2 level, and according to the previous discussion, they have an accuracy comparable to CCSD. A reevaluation of these quantities at the CCSD(T) level is prohibitively expensive, and thus we adopt the data from ref 24 for our work. The zero point energies, solvent effects, standard state corrections, and entropy changes are collected in Tables S4 and S5 of the Supporting Information, and in Table 2 we only list their sums. In this work, we also consider a so-called "explicit hydrogen bond correction" (EHBC) to the implicit solvent model.[47]

The solvent effects were computed by the conductor-like screening model (COSMO).[48] However, like all implicit solvent models, COSMO cannot treat the explicit, strong interactions between the solute and bulk solvent. Due to this reason one has to include explicitly the first hydration sphere of the lanthanoid(III) ions in the computations. However, even in this case there are still "dangling" O−H bonds left at the surface of lanthanoid(III) aqua complexes. If we define the difference of the number of dangling O−H bonds between the products and reactants as k, then by looking at Figure 1 and eq 1, we know that for $n = 8$, $k = 16 - 4 = 12$, and for $n = 9$, $k = 18 - 5 = 13$, when forming $Ln(H_2O)_n^{3+}$ from $(H_2O)_n^{3+}$ and Ln^{3+}. These O−H bonds will form hydrogen bonds with the bulk water, which are not accurately described by COSMO. To correct this error, we consider the following reaction, where $k = -1$:[47]

$$(H_2O)_8(aq) + H_2O(aq) \rightarrow (H_2O)_9(aq) \tag{3}$$

For a perfect modeling of bulk water the energy change of this reaction should be exactly zero. We computed the energy change of this reaction at COSMO/HF/aug-cc-pVTZ level, obtaining $\Delta E = -4.22$ kJ/mol. Thus, for the COSMO model, we estimate the EHBC to be $-4.22k$ kJ/mol. Now, adding this EHBC and thermodynamical and solvent effects to the binding energies, we obtain the hydration Gibbs free energies ΔG_H of octa- and nona-aqua lanthanoid(III) complexes which are listed in Table 2. Then we averaged them with the Boltzmann factor $\exp(-\Delta G_H/RT)$. These final values, as well as experimantal[25] ΔG_H's, are listed in Table 2. The RMSD of the errors is only 25 kJ/mol. Then the calculated values are currently the most accurate first-principle hydration Gibbs free energies. The computational scheme outlined here can be applied to the hydration of all metals in the periodic table, especially the actinides, where experimental data are very rare.

dx.doi.org/10.1021/ic500991x | Inorg. Chem. 2014, 53, 7700−7708

The hydration Gibbs free energies alone cannot give direct information on the preference of CNs. Ciupka et al. in ref 24 thus considered the reaction:

$$\mathrm{Ln(H_2O)_n^{3+}\cdot(H_2O)(aq) \rightarrow Ln(H_2O)_{n+1}^{3+}(aq)} \quad (n = 7, 8) \tag{4}$$

which represents the transfer of one water molecule from the second hydration shell to the first one. The free energy change of this reaction can be used as a measure of the preference of CNs: positive values implying n and negative are $n + 1$. Since we proved that DFT underestimates the binding energy for ions of larger CNs, it tends to predict too small preferred CNs, e.g., 7 for La^{3+}. Switching to SCS-MP2, the preferred CN of each Ln^{3+} was determined as 9 and 8 for the elements before and after Eu^{3+}, respectively. Note that from many theoretical and experimental studies this turning point was predicted also to be Eu^{3+} by Cossy et al.[49] but to be Ho^{3+} by Persson et al.[10] For Sm^{3+}, Eu^{3+}, and Gd^{3+} reaction 4 with $n = 8$ has a free energy change close to zero; therefore, both CNs 8 and 9 are possible. These results are in excellent agreement with the experiments.[6] By CCSD(T) calculations, we proved that B3LYP and MP2 have similar accuracy and SCS-MP2 is nearly comparable with CCSD. However, B3LYP as well as MP2 cannot treat the subtle energy change of reaction 4 well. This reminds us again that results of DFT or even low-level ab initio correlation methods like MP2 should be viewed with caution. SCS-MP2 has been proved very accurate; thus, its prediction of CNs is reliable.

WAVE FUNCTION ANALYSES

The energy computations only give the value of preferred CNs but do not tell us why they are attained. It also tells us little about the exchange kinetics. Thus, we performed a variety of wave function analyses, where SCF wave functions obtained from B3LYP calculations were used. Before proceeding, we note that although we used f-in-core PPs for lanthanoids(III), the introduction of f orbitals would not change the results of these analyses significantly but cause significant computational difficulties. Previous studies showed that f-in-core PPs show reasonable results.[50] Also, 4f orbitals of lanthanoids have very small spatial extent, making them rather core-like. An evidence is that by the scalar-relativistic Wood–Boring method the $\langle r \rangle$'s of 4f, 5s, 5p, and 6s orbital of the $[Xe]4f^7 6s^2$ configuration of Eu are computed to be 0.49, 0.74, 0.87, and 2.43 Å,[51] respectively. Thus, we believe that our computations with implicit treatment of f orbitals by PPs can give a realistic picture of lanthanoid(III) aqua complexes.

Interaction Nature. The electron localization function (ELF) was introduced by Becke and Edgecombe.[43] A large value of ELF means that the electrons are more likely confined in that region of space and may imply the existence of core electrons, covalent bonds, or lone pairs. An overview of the ELF distribution for $La(H_2O)_9^{3+}$ is provided by the isovalue surfaces in Figure 3. Details can be found in the color filled maps of ELF in Figure 4. We observed that the topological structures of ELF in the region of all Ln–O bonds (Ln–O(8), Ln–O(9P), or Ln–O(9C)) are almost identical: The lone pairs of the water molecules are pointing toward the lanthanoid(III) ions, without being noticeably deformed. This implies that the lanthanoid(III)–water interactions are mainly of electrostatic nature. The lanthanoid(III) aqua complexes are thus mainly bound by the dipole-charge electrostatic interactions, thus explaining also the good performance of classical force field methods.[14,16]

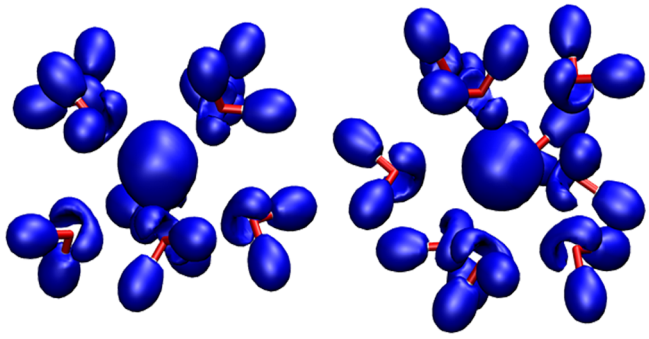

Figure 3. Isosurfaces (isovalue: 0.75) of ELF for $La(H_2O)_8^{3+}$ and $La(H_2O)_9^{3+}$. For other lanthanoids the graphs are very similar.

How much covalent contribution is present in the interaction? Here we consider a recently proposed bond order, i.e., the Laplacian bond order[52] (LBO)

$$\mathrm{LBO_{A,B}} = -10 \int_{\nabla^2\rho<0} w_A(\mathbf{r}) w_B(\mathbf{r}) \rho(\mathbf{r})\, \mathrm{d}\mathbf{r} \tag{5}$$

Here, A and B stand for atoms, ρ denotes the electron density, and w_A is a function determining the "region" of atom A by Becke's scheme.[53] In Figure 5A we plot the LBOs of Ln–O bonds. Equation 5 implies that only the points where $\nabla^2\rho < 0$ can contribute to LBO. It is well-known that $\nabla^2\rho < 0$ means that the electron density is locally concentrated, suggesting the existence of covalent interaction. Thus, LBO only reflects the covalent component of a bond. The LBOs of Ln–O bonds in lanthanoid(III) aqua complexes lie between 0.10 to 0.23 au (For the actual values see Table S6 of the Supporting Information). We note that LBOs of Na–F (ionic), C–F in CH_3F (polar covalent), C–H in CH_4 (unpolar covalent), and N–B in $H_3N{\cdot}BF_3$ (polar dative) are 0.06, 0.17, 0.89, and 0.24 au, respectively, at the B3LYP/aug-cc-pVTZ level. Thus, the covalent component of Ln–O bonds in aqua lanthanoids(III) is at the order of a typical ionic or polar dative bond.

In Figure 5B,C we plot bond lengths and LBOs versus their corresponding bond lengths (for bond lengths data see Table S7 of the Support Information). It is interesting to observe that the LBO is only determined by the bond length, being *independent* of what lanthanoid(III) or type of bond is involved. An exponential fitting with $R^2 = 0.9927$ between LBO and bond length r can be found:

$$\mathrm{LBO} = \mathrm{e}^{-3.6356(r-1.9427)} \tag{6}$$

This equation is very robust. For example, we optimized the geometry of $Ce(H_2O)^{3+}$, and the obtained Ce–O bond length is 2.30 Å. Substituting this into eq 6 we get a LBO of 0.27 au, which is almost identical with the exact value 0.27 au.

This again confirms that lanthanoid(III) aqua complexes are mainly electrostatically bound. The only reason for a larger LBO is the shorter Ln–O bond length which enables larger overlap of their orbitals. In fact, a natural bond orbital (NBO) analysis by Kuta and Clark with f-in-valence PPs also suggested that no covalent bonding was found between lanthanoid(III) ions and water except for $La(H_2O)_9^{3+}$ and $Lu(H_2O)_{8,9}^{3+}$.[23] Interestingly, while some other authors also claimed that La^{3+} can form slightly covalent bonding with water due to the (relatively) diffuse 4f orbitals,[54] Kuta and Clark according to their NBO analysis pointed out that these covalent bonds are

dx.doi.org/10.1021/ic500991x | Inorg. Chem. 2014, 53, 7700–7708

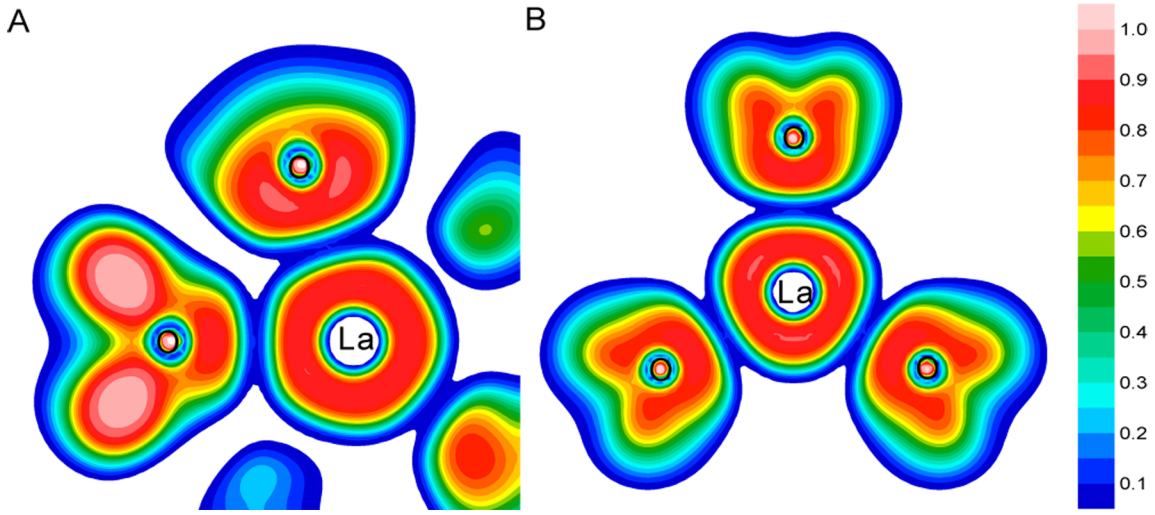

Figure 4. Filled color maps of ELF for $La(H_2O)_9^{3+}$ on (A) the plane of the lanthanum and two adjacent prism oxygen atoms; (B) the plane of three capping oxygen atoms. For other lanthanoids the graphs are very similar.

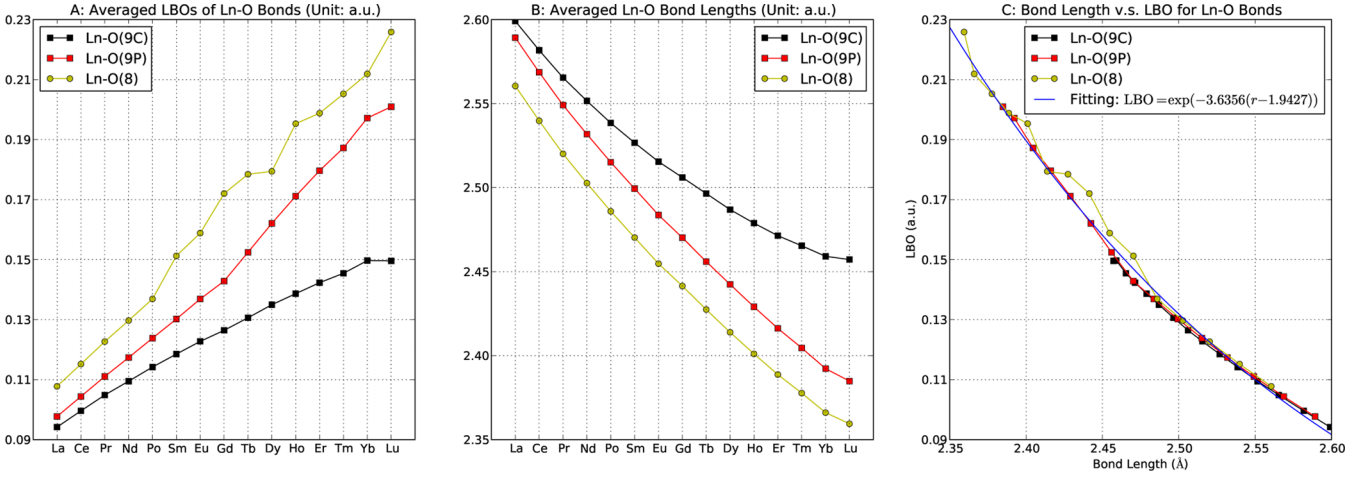

Figure 5. LBOs (A) and bond lengths (B) of Ln−O bonds in lanthanoid(III) aqua complexes. Their relationship and the fitting curve is shown in C.

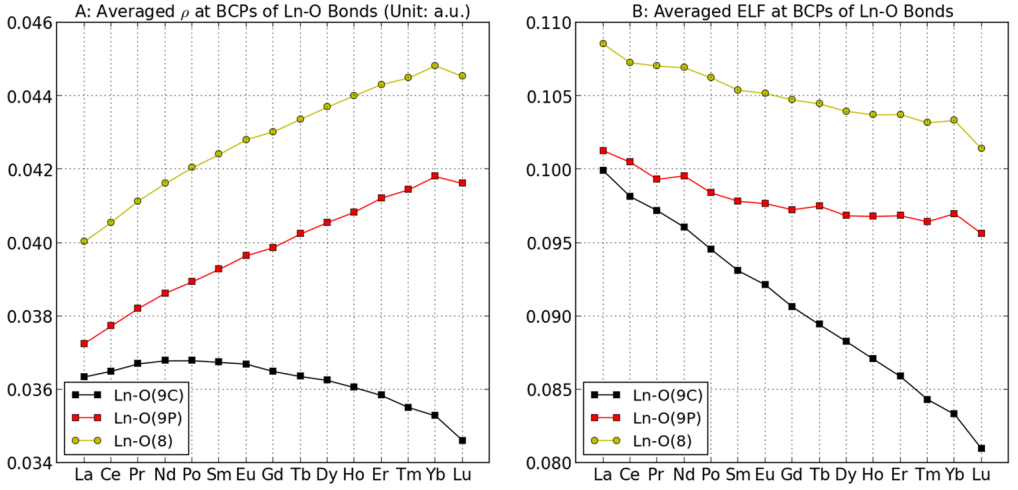

Figure 6. Averaged ρ (unit: a.u.) (A) and ELF (B) at BCPs of Ln−O bonds in lanthanoid(III) aqua complexes.

composed of 5% Ln p and d, and 95% O s and p orbitals, without contribution of f orbitals!

In order to obtain another qualitative estimate for the contributions to the binding energies we calculated at the HF level the $Ln(H_2O)_n^{3+}$ complexes as well as Ln^{3+} and $(H_2O)_n$ (n = 8, 9) fragments at the complex equilibrium geometries in the complex basis sets. The energy differences are estimates for the total interaction energies, not including the relaxation energies

dx.doi.org/10.1021/ic500991x | Inorg. Chem. 2014, 53, 7700−7708

of the $(H_2O)_n$ fragments when going from bulk water to the first hydration spheres of the ions. Calculations evaluating the first-order interaction energies of the fragments, i.e., orthogonalizing the Ln^{3+} and $(H_2O)_n$ orbitals and evaluating the HF expectation values without relaxing the orbitals, partition the interaction energies into a part comprising the electrostatic interactions as well as the Pauli repulsion between the fragments (between about 89% (88%) for lanthanum to 84% (82%) for lutetium, CN = 8 (9)) and a complementary part arising mainly from covalent interactions (see Table S8 of the Supporting Information for details). Thus, combining these findings with our ELF and LBO results, we conclude that there are only small covalent bonding contributions of about 10% to 20% between Ln^{3+} and water. The lanthanoid(III) aqua complexes are thus mainly bound by the dipole−charge electrostatic interactions.

Labile Capping Ln−O Bonds. The atom-in-molecule (AIM) theory was also applied in this work to analyze the Ln−O bonds. In Figure S1 of the Supporting Information we provide the molecular graphs. There exists exactly one bond critical point (BCP, yellow balls in Supporting Information Figure S1) for each Ln−O bond. The electron density at the BCP, ρ_{BCP}, is an important quantity in AIM theory. In Figure 6A (also see Table S9 of the Supporting Information), the averaged ρ_{BCP}'s of Ln−O bonds in lanthanoid(III) aqua complexes are shown.

It is often observed that the larger the ρ_{BCP} value is, the stronger the corresponding bond is.[55−57] Thus, a trend that ρ_{BCP} is larger for a shorter Ln−O bond is expected. This holds for both the Ln−O(8) and Ln−O(9P) bonds. However, the ρ_{BCP} of the Ln−O(9C) bonds exhibits a nonmonotonic behavior: it fluctuates between 0.0365 and 0.0367 au from La^{3+} to Sm^{3+} and then, more astonishingly, decreases from Sm^{3+} to Lu^{3+}, as the corresponding Ln−O(9C) bonds are getting shorter!

These ρ_{BCP}'s tell us that for the same Ln^{3+}, the Ln−O(8) bond is stronger than the Ln−O(9P) bond, which is stronger than Ln−O(9C); from La^{3+} to Lu^{3+}, the Ln−O(8) and Ln−O(9P) bonds become stronger in a parallel manner, while the Ln−O(9C) bonds remain somewhat constant in strength before Sm^{3+} and then get weaker. It is just after Sm^{3+} that the octa-aqua lanthanoid(III) complexes begin to be more stable. By realizing these facts we can understand the preference of CNs. There is a competition between the formation of eight Ln−O(8) and nine Ln−O(9) bonds in the water transferring reaction eq 4. For light lanthanoids, the Ln−O(9C) bond is strong enough that a nona-aqua complex is able to be bound; as going along the lanthanoid series, the Ln−O(9C) bond is getting labile, being easier to be disrupted by the environment. Thus, the heavy lanthanoid(III) complexes will switch to the more stable octa-aqua form.

The particularity of the capping bonds has been noticed before in the literature. In a study of $[Ln(H_2O)_9](CF_3SO_3)_3$ salts with crystallography and 2D solid state NMR a reduced occupancy of the three capping positions was observed for the heavier lanthanoid(III) ions Er−Lu.[58,59] Occupancies of 2.91, 2.96, 2.8, 2.7, and 2.4 water molecules were reported for Ho, Er, Tm, Yb, and Lu, respectively. Following older ideas[58,59] it was argued in a recent EXAFS spectroscopy and crystallography study of the same systems that the lanthanoid row should be partitioned into four tetrads intersecting at Nd/Pm, Gd, and Ho/Er.[10] In the first tetrad the capping bonds are relatively strong, whereas they get weaker in the second tetrad. In the third and fourth tetrads, due to the smaller ionic radius of the central ion and the increased repulsion between the water ligand, an asymmetry occurs and one capping bond gets stronger again, whereas the other two continue to become weaker. However, a corresponding difference in bond lengths was said to be too small to be detected by the EXAFS technique. The hydrated lanthanoid(III) ions in aqueous solution were said to be in this respect very similar to the salts.

Although we agree with the authors of these experimental studies that no abrupt structural change occurs at Gd, e.g., a gadolinium break due to reaching a half-filling of the 4f shell, and that the capping bonds play a special role, we do not have any evidence of the postulated asymmetry of the capping bonds for the heavier lanthanide(III) hydrates. Exploratory DFT calculations without imposing any symmetry restrictions on Lu^{3+} hydrates with one as well as two coordination spheres ($Lu^{3+}(H_2O)_9$, $Lu^{3+}(H_2O)_9(H_2O)_{18}$) did not give bond length differences larger than 0.01 Å for the capping bonds.

The present work provides a consistent and quantitative picture regarding the strengths of all Ln−O bonds in the equilibrium geometries, revealing a characteristic trend of the *labile capping Ln−O bonds*. This can explain the kinetics of the hydrated water molecules. Duvail et al. proposed that the exchange involves a bicapped trigonal prism (BTP) structure of octa-aqua lanthanoids.[12] This model can be supported and extended by our work, as illustrated by Figure 7. A water molecule at capping position is easier to exchange since the Ln−O(9C) bond is much weaker than the Ln−O(9P) or Ln−O(8) bonds. Thus, an octa-aqua complex which has a SAP structure will first rearrange to a BTP structure so that the water to exchange is on a capping position; for a nona-aqua ion, a prism water molecule will first rearrange to a capping position, and then it can exchange through a BTP intermediate. The possibility of a rearrangement between capping and prism water molecules has been confirmed by NMR experiments on crystals of $[Ln(H_2O)_9](CF_3SO_3)_3$.[58] Furthermore, these NMR studies reported that this rearrangement is already fast at 268 K for Lu^{3+} but becomes rapid only at about 300 K for La^{3+}, which can be explained by the strength of their Ln−O(9C) bonds. Now the unusual trend of water exchange rates can be understood. Since the Ln−O(9C) bond is relatively either very strong or very weak for light and heavy lanthanoids, respectively, once a nona- or octa-aqua ion forms, it will be very reluctant to dissociate a water molecule or rearrange to form a BTP intermediate. For the intermediate lanthanoids (from samarium to holmium), the Ln−O(9C) bond is of

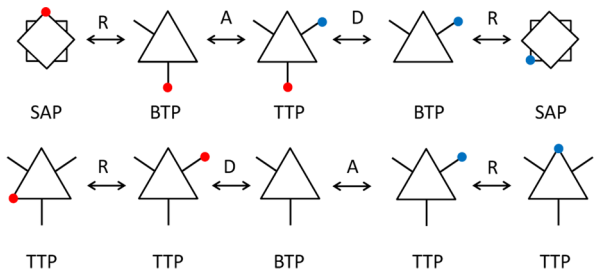

Figure 7. Water exchange mechanism. Other possible steps of association of a water molecule or rearrangement of a BTP intermediate for nona-aqua lanthanoids(III) are omitted for clarity. Circle: water molecule; A: association; D: dissociation; R: rearrangement.

dx.doi.org/10.1021/ic500991x | Inorg. Chem. 2014, 53, 7700−7708

moderate strength so it can readily both form and break, leading to a faster water exchange. Our model is also compatible with the I_a and I_d mechanism assumed by Helm and Merbach.[11] We also note that the nona- and octa-aqua lanthanoid(III) complexes can transform to each other through the BTP intermediate;[12] therefore, for intermediate lanthanoids, both nona- and octa-aqua ions can be long-lived, showing a fractional CN. Therefore, it is the strength of the capping Ln−O bond that determines the preferred CN, exchange rate, and perhaps other hydration behavior.

One would naturally wonder: why is a Ln−O(9C) bond weaker for a shorter bond length? The decreasing trend of Ln−O(9C) bond lengths on one hand can easily lead to a wrong conclusion regarding their strength, but on the other hand it is the key to explaining the abnormal behavior. From lanthanum to lutetium, the ionic radius decreases, leading to a higher electric field. Since we have proved that the lanthanoid(III) ions and water molecules mainly interact electrostatically, this decrease enhances the interaction between the water molecules and the lanthanoid(III) ions. Thus, the Ln−O(8) and Ln−O(9P) bonds get shorter and stronger in a parallel manner. This should also apply for the Ln−O(9C) bond. However, as shown in Figure 5B, the shortening of the Ln−O(9C) bond is much smaller than that of the Ln−O(9P) bond. This is the consequence of the fact that every capping water molecule will feel the strong repulsion from at least four neighboring prism ones. Thus, a short Ln−O(9C) bond indicates both large attraction with the lanthanoid(III) ion and large repulsion with the hydrated water molecules. For light lanthanoids (before samarium), the two factors are comparable and thus the strength of a Ln−O(9C) bond remains more or less constant. As the Ln−O(9P) bonds get short, the repulsion factor outperforms, depleting the electron density in the bonding region, and thus the Ln−O(9C) bonds begin to weaken. This picture can be confirmed by the ELF values at the BCPs in Figure 6B (also Table S10 of the Supporting Information), which shows that electrons are more and more unwilling to stay in the Ln−O(9C) region.

CONCLUSION

In this work, we systematically studied the lanthanoid(III) hydration from two aspects: energy and wave function. The highly accurate CCSD(T) method is for the first time applied to lanthanoid(III) aqua complexes via our recently developed inc3-db-B0 approach[29] which proves both accurate and efficient. These computations give accurate gas phase hydration energies and, more importantly, confirm the high accuracy of SCS-MP2, which is much faster than CCSD(T) and was used to optimize the structures and compute the hydration Gibbs free energies of lanthanoid(III) aqua complexes.[24] By correcting the explicit hydrogen bond error of COSMO and taking thermodynamic effects into account, we obtain so far the most accurate hydration Gibbs free energies from first principles. We believe that SCS-MP2, as well as the computational strategies proposed in ref 24 and this work, can be applied to, at least, any hydrated charged compound systems to get accurate energies. This is especially important for chemical species that lack experimental data.

The wave function analyses provide deeper insight for the hydration process. A striking fact revealed by AIM analysis is that a shorter capping Ln−O bond is weaker, at the first glance contrary to chemical intuition. By geometrical and ELF data, we prove that it is the larger repulsion from prism water molecules that weakens the capping Ln−O bond. Capping Ln−O bonds of moderate strength can form and break quickly and thus are advantageous to the formation of BTP intermediate during water exchange. This explains both the preferred CNs of lanthanoid(III) aqua complexes and the high water exchange rate for the middle region of the lanthanoid series. Thus, these labile capping Ln−O bonds determine most of the hydration behavior. We note that, for the study of hydration processes, some conclusions based solely on energies and geometrical parameters may be invalid. Instead, electronic structures and environmental factors (like water repulsion in this work, or counterions in solution) must be taken into account carefully in order to get a correct picture. Finally, we think that "labile capping bonds" might exist in other systems and could possibly also explain the kinetics of aqua complexes of other ions.

ASSOCIATED CONTENT

Supporting Information

The details of the hydration free energies, the magnitudes of LBO, ρ_{BCP}, ELF, energy decompositions, as well as Ln−O bond lengths, and the molecular graphs. This material is available free of charge via the Internet at http://pubs.acs.org.

AUTHOR INFORMATION

Corresponding Authors

*(J.Z.) E-mail: zhangjunqcc@gmail.com. Phone: ++49 (0)221-470-6893. Fax: ++49 (0)221-470-6896.

*(M.D.) E-mail: m.dolg@uni-koeln.de. Phone: ++49 (0)221-470-6893. Fax: ++49 (0)221-470-6896.

Notes

The authors declare no competing financial interest.

ACKNOWLEDGMENTS

The authors thank Dr. Jan Ciupka who provided us with the geometries and computational data of lanthanoid(III) aqua complexes and gave useful suggestions. The authors thank the Deutsche Forschungsgemeinschaft (DFG) for support.

REFERENCES

(1) Chen, J.; Zhu, Y.; Jiao, R. *Sep. Sci. Technol.* **1996**, *31*, 2723−2731.
(2) Dam, H. H.; Reinhoudt, D. N.; Verboom, W. *Chem. Soc. Rev.* **2007**, *36*, 367−377.
(3) Chan, K. W.-Y.; Wong, W.-T. *Coord. Chem. Rev.* **2007**, *251*, 2428−2451.
(4) Terreno, E.; Castelli, D. D.; Viale, A.; Aime, S. *Chem. Rev.* **2010**, *110*, 3019−3042.
(5) Pérez-Mayoral, E.; Negri, V.; Soler-Padrós, J.; Cerdán, S.; Ballesteros, P. *Eur. J. Radiol.* **2008**, *67*, 453−458.
(6) D'Angelo, P.; Spezia, R. *Chem.−Eur. J.* **2012**, *18*, 11162−11178.
(7) Choppin, G. R.; Graffeo, A. J. *Inorg. Chem.* **1965**, *4*, 1254−1257.
(8) Bertha, S. L.; Choppin, G. R. *Inorg. Chem.* **1969**, *8*, 613−617.
(9) Helm, L.; Merbach, A. *Coord. Chem. Rev.* **1999**, *187*, 151−181.
(10) Persson, I.; D'Angelo, P.; De Panfilis, S.; Sandström, M.; Eriksson, L. *Chem.−Eur. J.* **2008**, *14*, 3056−3066.
(11) Helm, L.; Merbach, A. E. *Chem. Rev.* **2005**, *105*, 1923−1960.
(12) Duvail, M.; Spezia, R.; Vitorge, P. *ChemPhysChem* **2008**, *9*, 693−696.
(13) D'Angelo, P.; Barone, V.; Chillemi, G.; Sanna, N.; Meyer-Klaucke, W.; Pavel, N. V. *J. Am. Chem. Soc.* **2002**, *124*, 1958−1967.
(14) D'Angelo, P.; Zitolo, A.; Migliorati, V.; Chillemi, G.; Duvail, M.; Vitorge, P.; Abadie, S.; Spezia, R. *Inorg. Chem.* **2011**, *50*, 4572−4579.
(15) Duvail, M.; Souaille, M.; Spezia, R.; Cartailler, T.; Vitorge, P. *J. Chem. Phys.* **2007**, *127*, 034503.
(16) Duvail, M.; Vitorge, P.; Spezia, R. *J. Chem. Phys.* **2009**, *130*, 104501.

(17) Dolg, M.; Cao, X. *Chem. Rev.* **2012**, *112*, 403−480.
(18) Dolg, M.; Stoll, H.; Savin, A.; Preuss, H. *Theor. Chim. Acta* **1989**, *75*, 173−194.
(19) Cao, X.; Dolg, M. *J. Chem. Phys.* **2001**, *115*, 7348−7355.
(20) Cao, X.; Dolg, M. *J. Mol. Struct. (THEOCHEM)* **2002**, *581*, 139−147.
(21) Clark, A. E. *J. Chem. Theory Comput.* **2008**, *4*, 708−718.
(22) Buzko, V.; Sukhno, I.; Buzko, M. *J. Mol. Struct: (THEOCHEM)* **2009**, *894*, 75−79.
(23) Kuta, J.; Clark, A. E. *Inorg. Chem.* **2010**, *49*, 7808−7817.
(24) Ciupka, J.; Cao-Dolg, X.; Wiebke, J.; Dolg, M. *Phys. Chem. Chem. Phys.* **2010**, *12*, 13215−13223.
(25) Marcus, Y. *Biophys. Chem.* **1994**, *51*, 111−127.
(26) Grimme, S. *J. Chem. Phys.* **2003**, *118*, 9095−9102.
(27) Stoll, H. *Chem. Phys. Lett.* **1992**, *191*, 548−552.
(28) Friedrich, J.; Hanrath, M.; Dolg, M. *J. Chem. Phys.* **2007**, *126*, 154110.
(29) Zhang, J.; Dolg, M. *J. Chem. Theory Comput.* **2013**, *9*, 2992−3003.
(30) Bader, F. W. *Atoms in Molecules: A Quantum Theory*; Oxford University Press: New York, 1994; p 1.
(31) Dunning, T. H. *J. Chem. Phys.* **1989**, *90*, 1007−1023.
(32) Yang, J.; Dolg, M. *Theor. Chem. Acc.* **2005**, *113*, 212−224.
(33) Zhang, J.; Dolg, M. *J. Chem. Phys.* **2014**, *140*, 044114.
(34) Yang, J.; Chan, G. K.-L.; Manby, F. R.; Schütz, M.; Werner, H.-J. *J. Chem. Phys.* **2012**, *136*, 144105.
(35) Riplinger, C.; Sandhoefer, B.; Hansen, A.; Neese, F. *J. Chem. Phys.* **2013**, *139*, 134101.
(36) Miliordos, E.; Aprà, E.; Xantheas, S. S. *J. Chem. Phys.* **2013**, *139*, 114302.
(37) Xantheas, S. S.; Aprà, E. *J. Chem. Phys.* **2004**, *120*, 823−828.
(38) James, T.; Wales, D. J.; Hernández-Rojas, J. *Chem. Phys. Lett.* **2005**, *415*, 302−307.
(39) Werner, H.-J.; et al. *MOLPRO*, version 2012.1, a package of ab initio programs; 2012. See http://www.molpro.net.
(40) Neese, F. *Wiley Interdiscip. Rev.: Comput. Mol. Sci.* **2012**, *2*, 73−78.
(41) Stephens, P. J.; Devlin, F. J.; Chabalowski, C. F.; Frisch, M. J. *J. Phys. Chem.* **1994**, *98*, 11623−11627.
(42) Frisch, M. J.; Trucks, G. W.; Schlegel, H. B.; Scuseria, G. E.; Robb, M. A.; Cheeseman, J. R.; Montgomery, J. A., Jr.; Vreven, T.; Kudin, K. N.; Burant, J. C.; Millam, J. M.; Iyengar, S. S.; Tomasi, J.; Barone, V.; Mennucci, B.; Cossi, M.; Scalmani, G.; Rega, N.; Petersson, G. A.; Nakatsuji, H.; Hada, M.; Ehara, M.; Toyota, K.; Fukuda, R.; Hasegawa, J.; Ishida, M.; Nakajima, T.; Honda, Y.; Kitao, O.; Nakai, H.; Klene, M.; Li, X.; Knox, J. E.; Hratchian, H. P.; Cross, J. B.; Bakken, V.; Adamo, C.; Jaramillo, J.; Gomperts, R.; Stratmann, R. E.; Yazyev, O.; Austin, A. J.; Cammi, R.; Pomelli, C.; Ochterski, J. W.; Ayala, P. Y.; Morokuma, K.; Voth, G. A.; Salvador, P.; Dannenberg, J. J.; Zakrzewski, V. G.; Dapprich, S.; Daniels, A. D.; Strain, M. C.; Farkas, O.; Malick, D. K.; Rabuck, A. D.; Raghavachari, K.; Foresman, J. B.; Ortiz, J. V.; Cui, Q.; Baboul, A. G.; Clifford, S.; Cioslowski, J.; Stefanov, B. B.; Liu, G.; Liashenko, A.; Piskorz, P.; Komaromi, I.; Martin, R. L.; Fox, D. J.; Keith, T.; Al-Laham, M. A.; Peng, C. Y.; Nanayakkara, A.; Challacombe, M.; Gill, P. M. W.; Johnson, B.; Chen, W.; Wong, M. W.; Gonzalez, C.; Pople, J. A. *Gaussian 03*, revision C.02; Gaussian, Inc.: Wallingford, CT, 2003.
(43) Becke, A. D.; Edgecombe, K. E. *J. Chem. Phys.* **1990**, *92*, 5397−5403.
(44) Lu, T.; Chen, F. *J. Comput. Chem.* **2012**, *33*, 580−592.
(45) Mardirossian, N.; Lambrecht, D. S.; McCaslin, L.; Xantheas, S. S.; Head-Gordon, M. *J. Chem. Theory Comput.* **2013**, *9*, 1368−1380.
(46) Boys, S.; Bernardi, F. *Mol. Phys.* **1970**, *19*, 553−566.
(47) Weißmann, D. *Personal communication*.
(48) Klamt, A.; Schüürmann, G. *J. Chem. Soc., Perkin Trans. 2* **1993**, 799−805.
(49) Cossy, C.; Helm, L.; Powell, D. H.; Merbach, A. E. *New J. Chem.* **1995**, *19*, 27−35.
(50) Dolg, M.; Stoll, H. In *Handbook on the Physics and Chemistry of Rare Earths*; Gschneidner, K. A., Jr., Eyring, L., Eds.; Elsevier Science B.V.: Amsterdam, 1996; Vol. 22.
(51) (a) Froese-Fischer, C. *The Hartree−Fock Method for Atoms - a Numerical Approach*; John Wiley & Sons, 1976. (b) Dolg, M. *Program MCHF*, modified version for pseudopotential and quasirelativistic calculations; 1987.
(52) Lu, T.; Chen, F. *J. Phys. Chem. A* **2013**, *117*, 3100−3108.
(53) Becke, A. D. *J. Chem. Phys.* **1988**, *88*, 2547−2553.
(54) David, F. H.; Vokhmin, V. *J. Phys. Chem. A* **2001**, *105*, 9704−9709.
(55) Grabowski, S. J.; Sokalski, W. A.; Leszczynski, J. *J. Phys. Chem. A* **2005**, *109*, 4331−4341.
(56) Domagała, M.; Grabowski, S. J. *J. Phys. Chem. A* **2005**, *109*, 5683−5688.
(57) Hugas, D.; Simon, S.; Duran, M. *J. Phys. Chem. A* **2007**, *111*, 4506−4512.
(58) Abbasi, A.; Lindqvist-Reis, P.; Eriksson, L.; Sandström, D.; Lidin, S.; Persson, I.; Sandström, M. *Chem.−Eur. J.* **2005**, *11*, 4065−4077.
(59) Wheelwright, E. J.; Spedding, F. H.; Schwarzenbach, G. *J. Am. Chem. Soc.* **1953**, *75*, 4196−4201.